RSC Advances

ROYAL SOCIETY OF CHEMISTRY

www.rsc.org/advances

Journal Name

ARTICLE

Bio-inspired polydopamine functionalization of carbon fiber for improving the interfacial adhesion of polypropylene composites

Received 00th January 20xx,
Accepted 00th January 20xx

DOI: 10.1039/x0xx00000x

www.rsc.org/

Yuan Liu [a], Yichao Fang [a], Jianhua Qian [b], Zuozhen Liu [b], Bin Yang [a,*] and Xinling Wang [a]

A simple and effective modification for carbon fiber (CF) were presented in this work. CF was functionalized with polydopamine (PDA) layer by pH-induced and oxidative self-polymerization of dopamine through a facile dip-coating procedure. The microstructure and chemical characteristics of CF surface before and after modification were investigated by SEM, AFM, IR, Raman, XPS and DCA. The results manifested that PDA functionalization could increase the roughness, polarity and wettability of the CF surface, which were advantageous to promote the interaction between CF and matrix. The interfacial propeties of single modified CF (dCF) and pristine CF with resins were measured by micro-droplet method. The interfacial shear strength (IFSS) of single dCF with maleic anhydride grafted PP (MAPP) modified polypropylene (PP) matrix was 284.3% higher than that of PP/CF. Both the dCF and pristine CF were also used to prepare PP composites and their mechanical properties were discussed in detail. PP/MAPP/dCF composite achieved a combination of excellent flexural and impact properties. The ultimate flexural strength and impact energy were increased by 105.0% and 223.0%, respectively. The excellent bulk performance was concluded to be mainly due to the superior interfacial adhesion obtained by covalent reaction and hydrogen bonding between PDA on CF and MAPP in PP matrix, which was also confirmed by the dynamic mechanical analysis (DMA) and fracture morphology observations.

1. Introduction

Carbon fiber (CF), as a very important reinforcing fiber for thermoset and thermoplastic composite materials, has been widely used in aerospace, sports and automobile industries, owing to its high specific strength, specific modulus, lower density and outstanding thermo-physical properties.[1] In recent years, vehicle materials increasingly focus on thermoplastic composites, because of their lower lightweight index, shorter cycle times and greater potential recyclability compared to thermoset polymers.[2] Among the general thermoplastic polymers, polypropylene (PP) has the lowest density and the largest consumption, due to its good comprehensive performance and versatile applications. Therefore, CF reinforced PP composites were extensively studied.[3-5]

It is well known that the ultimate performance of the resulting composites is closely related to the interfacial interaction between fibers and matrix. However, the smooth and chemically inert CF surfaces usually result in poor compatibility and weak interaction with low-polar PP. Thereby, excellent fiber-matrix interfacial adhesion strength could not be expected. Hence, research on improving the interfacial properties has been critical for developing high-performance CF reinforced composites.

Various methods have been reported to modify the CFs in order to increase the surface energy, induce chemically active functional groups, or change the surface microstructure, including wet oxidation,[6] electrochemical oxidation,[7,8] plasma etching,[9] chemical vapor deposition,[10,11] polymeric sizing or coating,[12-15] chemical grafting,[16,17] and so on. While, most of the above methods have certain limitations, such as tedious steps, drastic reaction conditions, high toxicity, or serious damage to the structure and strength of fiber itself. Thus, the development of a facile, effective and green strategy for the CF surface functionalization is highly desirable.

Recently, bio-inspired dopamine which can self-polymerize under extremely mild conditions and generate adhesive polydopamine (PDA) coating onto almost all types of materials has attracted much attention.[18] The dopamine functionalization approach has been particularly preferred for the advantages of easy operation through soaking substrates in pH 8.5 dopamine solutions at room temperature and controllability by dopamine concentration or reaction time. Furthermore, the strongly adhered PDA layer could be used as a versatile platform for secondary reactions. The residual amino and catechol groups of PDA can form chemical bridges or hydrogen bonds with the specific functional groups of other polymers, making PDA an effective stress transfer agent at the interfaces.[19] In the past few years, various substrates, such as clay,[20-22] plastics,[23] graphene oxide,[24] and nanotubes[25] have been surface-modified with PDA using the above mentioned method.

[a] State Key Laboratory of Metal Matrix Composites, School of Chemistry & Chemical Engineering, Shanghai Jiao Tong University, 800 Dongchuan Road, Shanghai, 200240, China. E-mail: byang@sjtu.edu.cn; Tel: +86 21 54742566
[b] Huachang Polymer CO.,LTD., 130 Meilong Road, Shanghai, 200237, China.

In this study, we aimed to enhance the interfacial characteristics between CF and PP matrix through modifying CF with this novel PDA via a simple one-step dip-coating method. CF functionalized with PDA were thoroughly characterized by SEM, AFM, XPS, IR, Raman and DCA. The smooth and inert surface of CF was converted to be rough, active and wettable by resin after coating with a PDA film. We further improved the interfacial adhesion of CF and matrix by modifying the polymeric matrix with strong-polar compatibilizer. Maleic anhydride grafted polypropylene (MAPP) proved to be an effective compatibilizer in fiber reinforced PP plastics.[26,27] Given this, we made use of the chemical reaction between PDA on CF surface and MAPP in PP matrix to further improve the interface performance.

To evaluate the efficiency of PDA coating in combination with MAPP modification on the improvement of interfacial interaction, we incorporated the PDA functionalized CF and pristine CF into PP or PP/MAPP resins and investigated the interfacial shear strength, macro-performance and fracture morphology. The satisfactory effect was identified by the excellent interface performance between functionalized CF and modified PP matrix, indicating that this simple strategy was efficient and PDA was able to form a strong interfacial bonding to connect fibers and resin so as to achieve remarkably improved mechanical properties.

2. Experimental details

2.1 Materials

PP pellets (Y2600T, MFR=26, Petroleum & Chemical, China) and CF (T700SC 12K, Toray, Japan) were used as the polymer matrix and the reinforcing material. Dopamine hydrochloride (Sigma, Shanghai) served as the fiber modifier and tris (hydroxylmethyl) aminomethane (Tris, Aladdin, Shanghai) was used as received. Maleic anhydride grafted PP (MAPP, SUNNY, Shanghai) with a MAH content of 1.0 wt% was used as a compatibilizer.

2.2 Surface functionalization of CF

Dopamine solution (2 mg/ml) was prepared by dissolving dopamine in Tris-HCl buffer solution (10 mM, pH 8.5). Subsequently, CF bundles were immersed in dopamine solution at room temperature for 24 h. A thin PDA layer was adhered on CF surface via the oxidative self-polymerization of dopamine. Then, the polydopamine coated fibers (dCF for short) were taken out, washed with deionized water for several times until the solution was colorless and dried in a vacuum oven at 50 °C overnight.

Afterwards, to investigate the stability and the amount of the PDA coating, dCF was immersed in 0.1 M hydrochloric acid solution for different periods of time to reclaim the original CF, and the detachment was monitored by recording the UV absorbance. The PDA deposition mass was determined by calculating the weight loss of the dCF in strongly acidic condition.

2.3 Preparation of PP composites

Prior to the composites preparation, CF and dCF were chopped into an average length of 10 mm, and then dried in an oven at 70 °C for 12 h together with PP pellets. MAPP was used directly without drying. The melt blending of CF or dCF (30 wt%) with PP or PP/MAPP (20 wt% MAPP in PP) were carried out for 10 min by an internal mixer (Thermo Haake PolyDrive, USA). The rotor speed and temperature were set at 50 rpm and 190 °C, respectively. The compounds were then placed in a mould of size 10 cm× 10 cm × 2 mm and compressed using Platen Press Machine (XLB-D, Labtech, Germany) at 200 °C under a pressure of 15 MPa. At last, the composite sheets were cut into rectangular specimens of 100 mm × 10 mm × 2 mm using Waterjet Cutting Machine (Flow, USA) for mechanical tests. The composites were defined as PP/CF, PP/dCF, PP/MAPP/CF or PP/MAPP/dCF. Pure PP was also prepared and experienced the same thermal history described above for reference.

2.4 Characterization of carbon fibers

The UV–vis spectra of dopamine in solution were recorded on UV-1800 spectrophotometer (Shimadzu, Japan) using H_2O as solvent. All measurements were performed in quartz cuvettes. The light source wavelength was 340 nm and scan range was 200–600 nm.

To obtain the PDA amount on dCF surface, the thermal decomposition behaviors of CF, dCF, dopamine and PDA were investigated by Thermogravimetric Analyzer (Q5000IR, TA, USA) in the range of 40-800 °C at heating rate of 20 °C/min and N_2 flow rate of 40 ml/min.

The morphology of CF and dCF surface as well as fracture regions of PP composites after flexural tests were studied through a Scanning Electron Microscopy SEM (Nova NanoSEM 450, FEI, USA), with a 5 KV acceleration voltage. The fracture surfaces were sputter-coated with gold (Q150TS, Quorum, UK) before observation to avoid charging.

The surface morphology of CFs were also examined by Atomic Force Microscope AFM (Nanoscope IIIa Multimode, Digital Instruments, USA) height images using tapping mode.

Fourier Transform Infrared (FT-IR) spectra of fibers and composites were recorded on a Paragon 1000 FT-IR spectrometer (Perkin Elmer, USA). The scan range was 4000-400 cm^{-1} and four scans were collected for each sample with a resolution of 2 cm^{-1}.

The chemical composition and functional groups on CF and dCF surface were characterized by X-ray Photoelectron Spectroscopy XPS (AXIS Ultra DLD, Shimadzu, Japan) equipped with a monochromatic source of Al Kα (1486.6 eV), spot area of 700 μm × 300 μm, base pressure below 5×10^{-9} Torr, pass energy of 160 eV and 40 eV for survey scans and narrow scans, respectively. The binding energy peaks were calibrated with C1s at 284.8 eV as reference.

Raman spectra of CF and dCF were collected on a DXR Raman Microscope (Thermo Scientific, USA) with a 2 mW 532 nm excitation wavelength laser from 100 to 3500 cm^{-1}. The spectra were fitted with Lorentzian function.

Dynamic contact angles were measured to evaluate the wetting performance of CF and dCF on DCAT20 system (Dataphysics, Germany) by using Wilhelmy plate technique.[28] Five fibers were fixed on a card paper of 10 mm × 20 mm size and then immersed into the test liquid with a depth of 5 mm, advancing and receding speed of 0.008 mm/s. The contact angle θ was determined by Wilhelmy equation (1):

$$cos\ \theta = \frac{wg}{L\gamma} \quad (1)$$

where w is the weight detected by the DCAT20 system, L is the fiber wetted perimeter, γ is the surface tension of the test liquid. Deionized water (γ_L =72.8 mN/m, γ_L^p =51.0 mN/m, γ_L^d=21.8 mN/m) and diiodomethane (γ_L=50.8 mN/m, γ_L^p=2.3 mN/m, γ_L^d=48.5 mN/m) were used as test liquids, whose surface tensions γ_L, polar γ_L^p and dispersive γ_L^d components are already known. Owens double-liquid method was employed to calculate the surface free energies γ_S, polar components γ_S^p and dispersive components γ_S^d by solving the following equations (2) and (3):

$$\gamma_L(1+\cos\theta) = 2\sqrt{\gamma_S^p\gamma_L^p} + 2\sqrt{\gamma_S^d\gamma_L^d} \quad (2)$$

$$\gamma_S = \gamma_s^p + \gamma_S^d \quad (3)$$

In every sample, at least 10 different specimens were chosen and the results were averaged.

We employed the micro-droplet method to determine the interfacial shear strength (IFSS) of single fibers and resins using the interfacial evaluation equipment (MODEL HM410, Japan). One single CF (approximately 50 mm in length) was separated from the CF bundles, and two ends of which were fixed. The IFSS between the CF and matrix was calculated using the following equation (4):

$$IFSS = \frac{F_m}{\pi d_f L_e} \quad (4)$$

where F_m is the maximum tensile force, d_f is the fiber diameter and L_e is the fiber length embedded in the matrix. At least 30 valid data were collected and averaged for each sample.

2.5 Mechanical property testing of composites

Flexural tests of neat PP and PP composites were conducted by a Universal Testing Machine (Criterion 43, MTS, USA) with three-point bending (TPB) testing mode at a constant speed of 2.0 mm/min and a span length of 64 mm in accordance with ASTM D790. Unnotched Izod impact tests were performed on a Pendulum Impact Tester (RAY-RAN, UK) with striker energy of 5.01 J, according to the ASTM D256. At least five parallel samples were recorded for each specimen in both tests.

The dynamic mechanical performance of neat PP and PP composites were mearsured using a Dynamic Mechanical Analyser (DMA 242C, NETZSCH, Germany). Samples of 50 mm × 10 mm × 2 mm size were tested in three-point bending mode with a span of 40 mm, heating rate of 3 °C/min, maximum amplitude of 120 μm, and maximum dynamic force of 2 N at a frequency of 1 Hz within a temperature range of -40-100 °C.

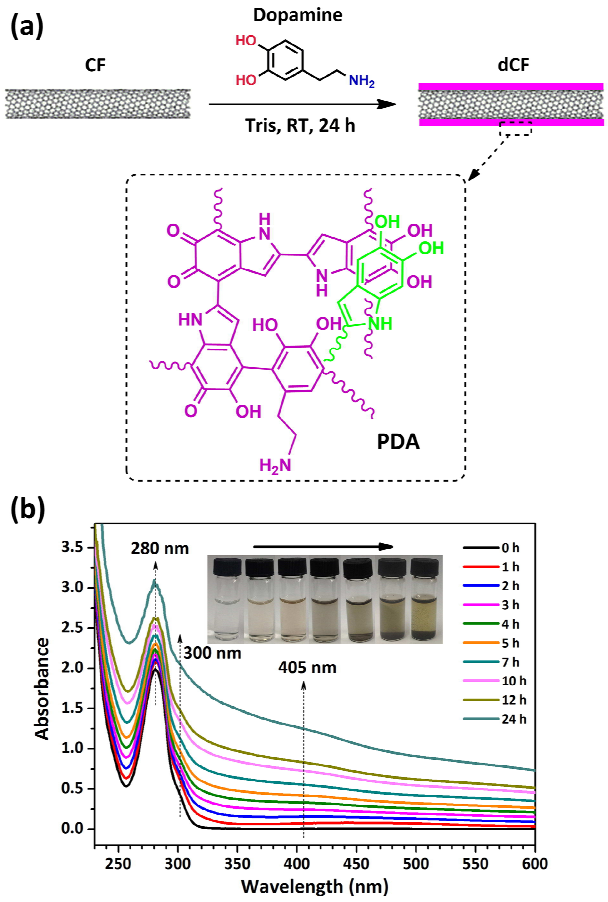

Fig. 1 (a) Schematic of the dipping process and the structure of PDA (b) UV–vis spectra of dopamine solution over time

3. Results and discussion

3.1 Surface topography of carbon fiber

In this study, pristine CF was simply dipped into a weak alkaline dopamine solution and mildly stirred at room temperature and polydopamine was expected to form via the oxidative polymerization of dopamine on the CF surface. The dipping process and PDA structure were schemed in Fig. 1a. According to L. Y. Jia's report, dopamine underwent the similar self-polymerization to produce polydopamine in both solution and substrate surface.[29] Therefore, the reaction process in solution was monitored using UV–vis spectroscopy to obtain some ideas of the spontaneous deposition of adherent polydopamine on fibers. As shown in Fig. 1b, the sharp absorbance peaks at 280 nm (catechol group), shoulder peaks at 300 nm (dehydro-dopamine) and wide peaks at 405 nm (o-quinone) were observed to increase in intensity over time,

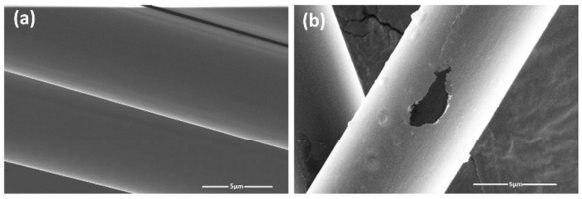

Fig. 2 SEM images of (a) pristine CF (b) dCF

which suggested the formation of various intermediates.[30] The inset digital images also presented the apparent color change (from pink to brown, then black) during the PDA formation.

The differences in surface morphology could be easily observed by SEM and AFM. PDA functionalized CF was thoroughly rinsed with water in ultrasonic cleaner and dried before observation to eliminate adsorbed molecules by weak physical interaction. The SEM images of pristine CF and PDA coated CF are shown in Fig. 2. The surface of pristine CF was perfectly smooth and clean (Fig. 2a). After impregnation, the fiber surface was uniformly covered by a thin layer. Fig. 2b was chosen on purpose, for the defect with curled edges on dCF remarkably revealed the presence of PDA coating.

The three-dimensional and two-dimensional AFM images (Fig. 3) also indicated a rougher surface of dCF, compared to that of pristine CF. The PDA layer on dCF slightly altered the surface average roughness (Ra) from 35 nm to 47 nm. The increase in surface roughness would lead to higher surface area and was expected to enhance mechanical interlocking between the fiber and matrix.

TG analysis was employed to evaluate the PDA amount coated onto the fibers during dipping process. As Fig. 4a shown, pristine CF showed no obvious weight loss (only 0.7 wt%), consistent with its excellent thermal stability. The residual mass of PDA homopolymer was about 40 wt% up to 800 °C, indicating a higher thermal stability than dopamine monomer. In detail, PDA exhibited a three-step weight loss

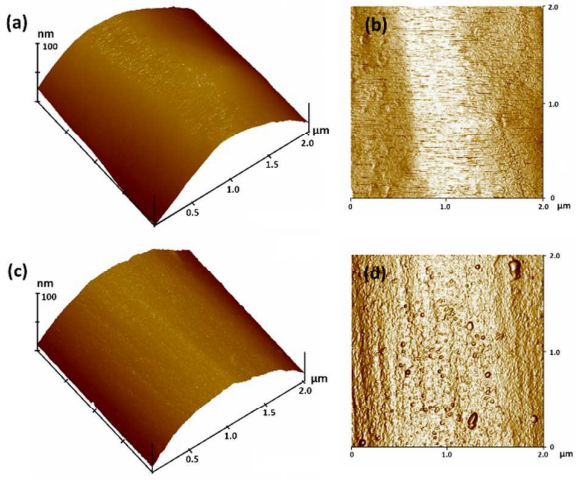

Fig. 3 AFM 3D and 2D height images of (a, b) pristine CF and (c, d) dCF

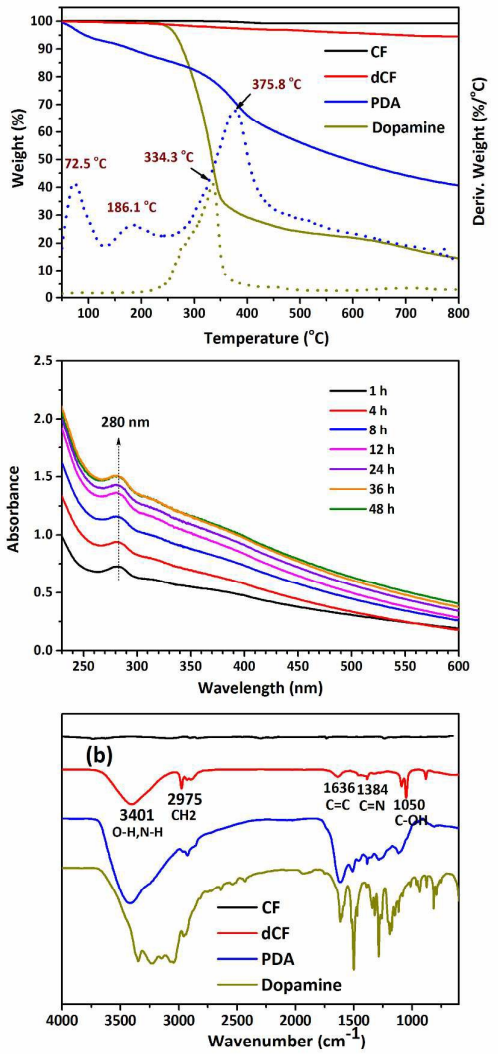

Fig. 4 TGA (a) and FT-IR spectra (c) of pristine CF, dCF, PDA and dopamine, (c) UV-vis spectra of HCl solution after dipping the dCF

process. The first mass loss at 72.5 °C was attributable to the elimination of moisture and other residuals. The second loss at 186.1 °C could be ascribed to the breakage of catechol moiety and amine groups. While, the major degradation occurred at 375.8 °C, corresponding to the decomposition of the PDA main chains. The 5 wt% mass loss of dCF proved PDA was successfully deposited onto the CF and its mass fraction was calculated to be about 6.7 wt%.

We further evaluated the amount and chemical stability of PDA coating by immersing dCF in 0.1 M HCl solution. The UV absorbance of the acidic solution was then measured as Fig. 4b. The absorbance peak intensity at 280 nm and ill-defined broad peaks increased as time extended and remained essentially unchanged after 36 h. This was most probably due to the dissolution of unreacted monomers or small oligomers, the degradation of PDA into structural units as well as PDA

that were weakly bound to CF surface via non-covalent interactions when exposed to strongly acidic environment. Based on the mass change, only 3.5 wt% detached polymer was detected within 48 h. The value was lower than the above TGA data, which proved that PDA deposited on CF was partially stable in strongly acidic solution.

3.2 Surface chemical structure of carbon fiber

FT-IR was used to determine the chemical group changes on CF surface. Before measurement, dCF were ultrasonically rinsed three times to eliminate residual dopamine monomer and physically adsorbed polydopamine homopolymer. Fig. 4c shows the FT-IR spectra of pristine CF, dCF, PDA and dopamine. Almost no obvious peaks were detected on pristine CF, which could be attributed to the low transmittance of black materials and tiny content of sizing agent. Upon coating with PDA, some major bands were distinctly observed on the dCF spectrum. A strong and broad absorption band around 3401 cm^{-1} arose from the catechol O-H and N-H stretching vibrations. While peaks around 2975 cm^{-1} were due to C-H stretching vibrations. The single absorption band at 1636 cm^{-1} was attributed to aromatic C=C from PDA layer. The new absorption peak of dCF at 1384 cm^{-1} was assigned to the shearing vibration of aromatic C=N groups. Peaks at 1090 cm^{-1} and 1050 cm^{-1} were the characteristic absorption peaks of C-OH. The bands found on dCF were consistent with PDA homopolymer and dopamine. Therefore, IR provides further evidence that dopamine has been polymerized onto CF surface. The mechanism of dopamine polymerization has been clearly demonstrated by W. Y. Kim et al.[31] They identified that polydopamine was formed through non-covalent self-assembly and covalent polymerization.

Raman spectroscopy can provide rich information on the ordered/disordered structure of the near-surface region of carbon materials. As shown in Fig. 5, the Raman spectrum of CF displayed three main characteristic peaks, which are important indicators of the structural defects in carbon-based materials. The D peak at 1361 cm^{-1} is associated with amorphous carbon atoms (sp^3-hybridized), activated by some defects, such as edges, functional groups or structural disorders. The G-band at 1592 cm^{-1} is intrinsic of graphitic structure, corresponding to a well-defined sp^2-bonded carbon type. In the second-order Raman spectrum, the band around 2670 cm^{-1} is designated as the G´ band (or 2D). It was induced by a double-resonance effect and also the overtone of the D band. The sharp G´ peak was always obtainable in almost defect-free samples.[32,33] Thus, as a low-ordered graphitic material, CF showed a strongly dispersive G´ band. The integral area ratio of D peak intensity to G peak intensity (I_D/I_G) was conveniently used to assess the degree of graphitization. Thus, a higher I_D/I_G ratio indicates more defects and disorders of the graphitic materials.[34,35] Similar peaks at D band (1361 cm^{-1}) and G band (1601 cm^{-1}) were also observed in the Raman curve of dCF. It can be found that the locations of D and G bands were nearly unchanged, implying that dipping process did not affect the entity structure of pristine CF. While the I_D/I_G ratio increased from 1.95 to 2.20. The higher I_D/I_G ratio of dCF suggested the formation of PDA molecules, which increased the degree of disorder and the amorphous carbon atom number of CF surface.

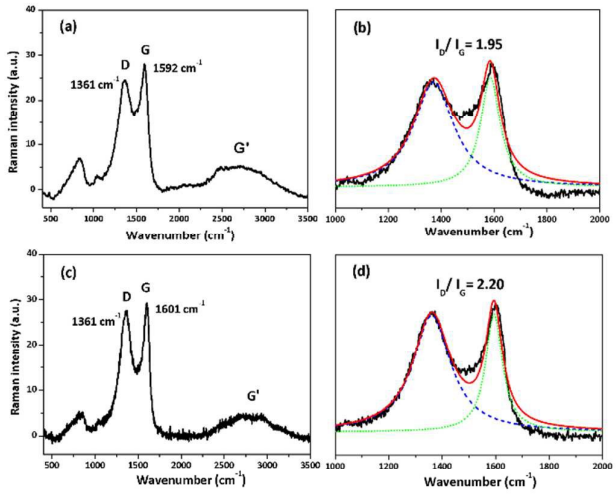

Fig. 5 Raman spectra and fitted curves of (a, b) pristine CF and (c, d) dCF

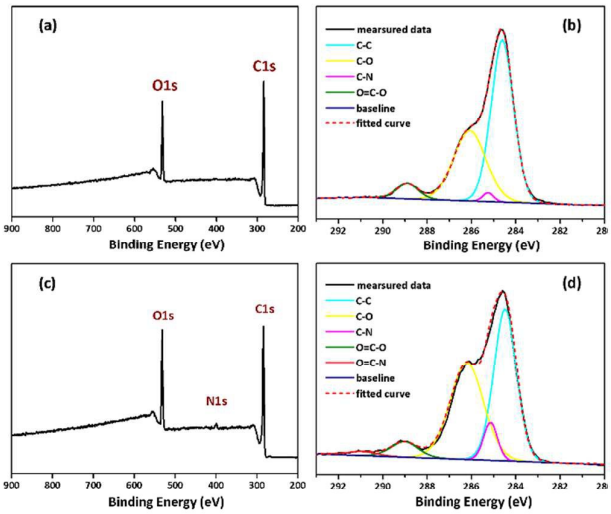

Fig. 6 XPS spectra and C1s peak-fitting curves of (a, b) CF and (c, d) dCF

XPS was used to investigate the chemical compositions of CF surfaces. Fig. 6 shows the XPS wide-scan and C1s spectra of CF and dCF, in which the C1s peaks were further curved-fitted with four or five components, assigned to C-C (284.7 eV), C-N (285.4 eV), C-O (286.2 eV), O=C-O (289.0 eV), and O=C-N (290.9 eV), respectively.[36] The surface element compositions from XPS wide survey and functional components obtained from the deconvolution of C1s peaks are listed in Table 1. Compared with pristine CF, the atom percentage of N1s on dCF surface dramatically ranged from 0.8% to 2.1%, and the

Table 1 Surface element and functional group compositions of CF and dCF

Samples	Element composition (%)					Functional group composition (%)				
	C_{1s}	O_{1s}	N_{1s}	O_{1s}/C_{1s}	N_{1s}/C_{1s}	C-C	C-N	C-O	O=C-O	O=C-N
CF	83.6	15.6	0.8	0.19	0.01	59.0	1.4	35.6	4.0	-
dCF	80.0	17.9	2.1	0.22	0.03	44.5	6.7	41.7	5.5	1.6

Table 2 Contact angles and surface energies of CF and dCF

Samples	Dynamic contact angles (°)		Surface energies (mJ/m^2)		
	θ_{water}	$\theta_{diiodomethane}$	γ_S	γ_S^p	γ_S^d
CF	83.08	84.23	23.4	13.0	10.4
dCF	73.48	82.52	29.8	19.9	9.9

percentage of C-N was largely increased from 1.4% to 6.7%. Besides, dCF showed a new bonding energy peaks at 290.9 eV (O=C-N), which all confirmed the existence of PDA containing rich amine groups. Meanwhile, dCF showed a higher oxygen concentration, O/C atomic ratio, as well as C-O and C=O percentages, due to the catechol and quinone groups of PDA polymer.

The higher content of oxygen-containing and amine functional groups on dCF were expected to increase the polarity and reactivity of the CF and supply more reactive sites for interfacial bonding, which would result in an improvement of the fiber-matrix interaction. Besides, the introduction of extra polar groups could affect the fiber surface energy, which is closely related to the wettability between fibers and matrix.

3.3 Surface free energy of carbon fiber

It is well known that high fiber surface energy can increase a better wettability between the CFs and the matrix. The surface energies of CFs were calculated via the contact angles between testing liquids and single fibers. The DCAT20 system recorded the wetting weight vs. immersion position (one example shown in Fig. 7) and the weight extrapolated value at zero immersion depth was used for determining the θ_{water} and $\theta_{diiodomethane}$ by solving the equation (1). The surface free energy γ_S and its two components (dispersive component γ_S^d and polar component γ_S^p) were obtained by equations (2) and (3). The detailed values are summarized in Table 2. Firstly, the change of the fiber surface free energy confirmed the chemical adhesion of PDA onto CF successfully. After the PDA modification, the total surface free energy showed an obvious rise from 23.4 mJ/m^2 to 29.8 mJ/m^2. This increase was mainly bought by its polar component, which was contributed by the massive functional groups supplied by PDA. While, the dispersive component γ_S^d shows little change after PDA functionalization. As we know, the dispersive component is dominated by the topography of fibers.[37] As presented above in Fig. 2, the roughness of dCF was only slightly higher than that of CF, due to the uniform distribution of PDA polymer layer on the fiber surface. Namely, the PDA functionalization did not give rise to enough visible change in CF surface morphology to alter the dispersive component obviously. The functional groups of PDA could increase the surface energy of the fiber reinforcement. Therefore, better wetting of fibers in the melted polymer was expected to achieve and the interfacial adhesion between coated fibers and matrix resin may be enhanced as well.

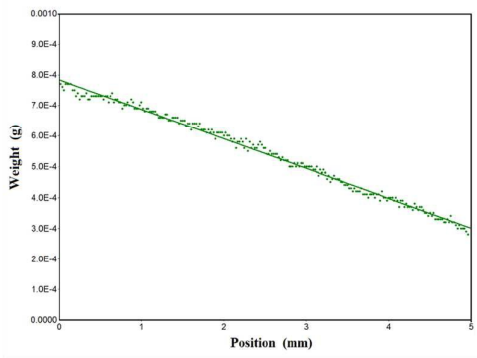

Fig. 7 A typical weight-position curve in the DCA experiment

3.4 Interfacial shear strength analysis

Micro-droplet tests were used to directly assess the interfacial properties between a single fiber and the resin.[38] Fig. 8 shows the interfacial shear strength (IFSS) results of single fibers with PP or PP/MAPP resin. The functionalization of PDA onto CF surface gave rise to an 88.2% improvement (from 4.84 MPa to 9.12 MPa) in IFSS in comparison with that of untreated CF and PP resin. The IFSS of PP/MAPP/CF was also 130.8% higher than that of PP/CF, because of the coupling effects of MAPP compatibilizer. What's more, the IFSS between dCF and

PP/MAPP reached up to 18.62 MPa, significantly improved by 284.3%, compared to that of raw CF and pure PP. The results revealed that CF surface functionalization by dopamine and PP matrix modified by MAPP greatly enhanced the interfacial adhesion of fiber/PP composite. We attribute this high interfacial enhancement to the chemical interaction between coated amine functional groups of PDA and maleic anhydride (MAH) groups of MAPP.

As discussed above, a homogeneous PDA layer was easily and successfully coated onto CF surface through a simple one-step dip-coating method, based on the above results of SEM, AFM and Raman. FT-IR, XPS and contact angles clearly proved that the attachment of PDA brought about more active functional groups and higher surface free energy onto the fiber. The rich functional groups of PDA increased the surface energy of dCF

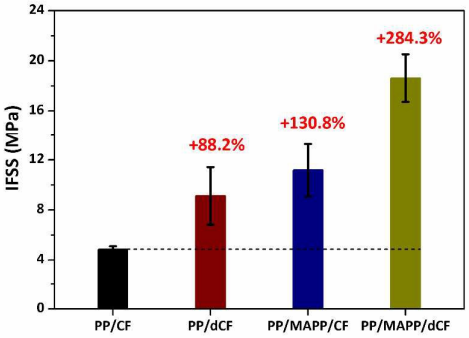

Fig. 8 IFSS of single fibers with resins

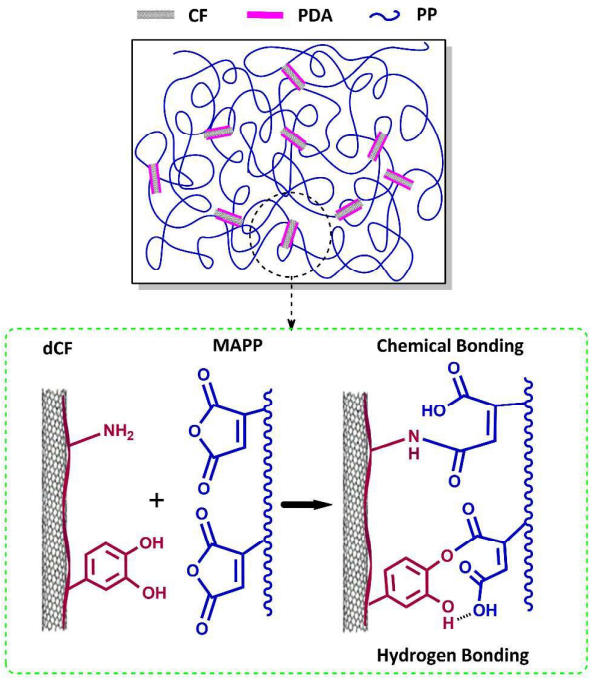

Fig. 9 Schematic of the interfacial interaction in PP/MAPP/dCF composite

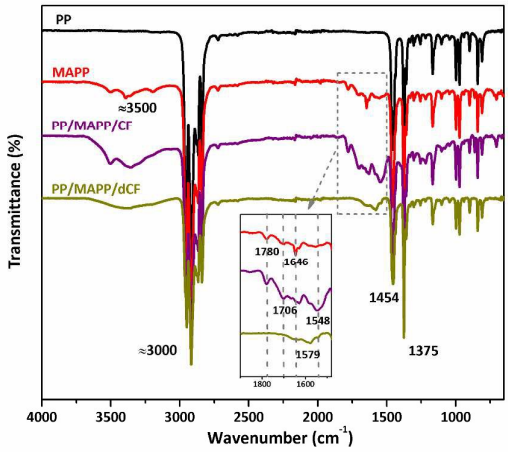

Fig. 10 FT-IR spectra of PP, MAPP and their composites

and made the surface easier to be wetted by polar resin (PP/MAPP), thus, leading to enhance the interfacial interaction of composites. Furthermore, the amine and catechol groups of PDA on fiber surface may react with maleic anhydride (MAH) groups in PP/MAPP matrix through ring-opening reaction during composites preparation (Schemed in Fig. 9), which would form strong chemical bonding at the interface of PP/MAPP/dCF composite. In addition, MAH groups were easily opened and turned into dicarboxylic acid groups during the high temperature melt mixing. Hence, hydrogen bonding might also be created with the amine groups between fibers and matrix, to improve the interfacial adhesion of composites.

The reaction mechanism was further proved by the FT-IR spectra of PP, MAPP, and their composites in Fig. 10. The multi-peaks near 3000 cm^{-1} were attributed to the C-H stretching vibration, while, the two intensive peaks at 1454 cm^{-1} and 1375 cm^{-1} were assigned to the C-H bending vibration of PP backbone, respectively. MAPP was observed to have similar absorption peaks as pure PP except additional peaks around 3500 cm^{-1} and multipeaks at 1800-1500 cm^{-1} (1780 cm^{-1}, 1706 cm^{-1}, 1646 cm^{-1}, 1548 cm^{-1}), which were apparently due to the O-H and C=O vibration of the MA groups, respectively. The characteristic peaks were observed to be well maintained in PP/MAPP/CF. However, most of them disappeared and a new broad peak at 1579 cm^{-1} appeared in PP/MAPP/dCF, indicating the formation of amido bond between dCF and PP/MAPP backbone.[39]

3.5 Static mechanical properties of composites

The PDA functionalization was confirmed to increase the interfacial adhesion of single CF filament and resin by IFSS, which would promote the macro-performance of CF reinforced PP composites. We further discussed the effectiveness of this modification on the ultimate mechanical performance of prepared materials in the following. The mechanical properties of neat PP and its composites (reinforced by 30 wt% fibers) are shown in Fig. 11. It was clearly visible that the addition of 30 wt% CF enhanced the flexural properties of PP to a large

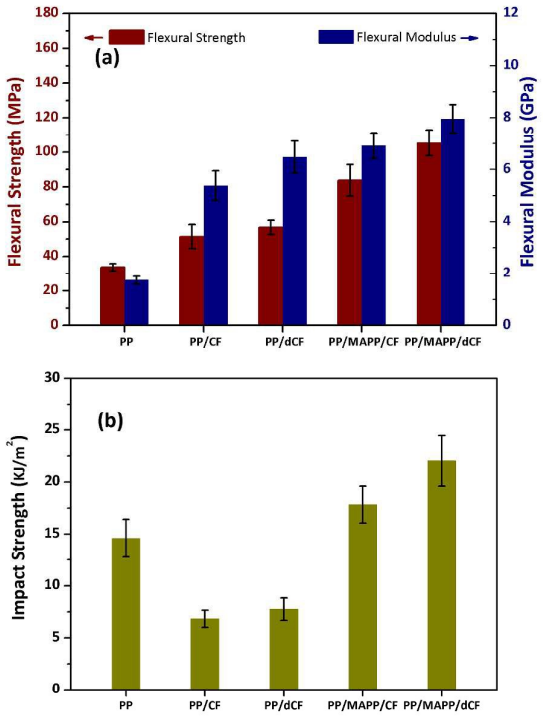

Fig. 11 Mechanical properties of neat PP and PP composites (a) flexural properties (b) impact properties

extent, while decreased its impact toughness. This result was reasonable because of CF's high strength and high modulus nature or stiffness and rigidity, which was consistent with Arbelaiz A's studies.[40] For another reason, the addition of CF created many stress concentrations that required less energy to initiate cracking, which led to the drop of impact strength. Compared with PP/CF, the improvement of PDA on the mechanical properties of PP/dCF was limited. For example, the flexural strength of PP/dCF composite was increased from 51.41 MPa to 56.83 MPa by only 10.5%. On account of the unimpressive roughness changes of dCF, the results indicated that the surface topography of CF was not the main factor responsible for the mechanical property of PP composites. Alternatively, the MAPP compatibilizer could also produce good mechanical behavior through its coupling effect between the CFs and PP matrix, confirmed by Z.H. Guo's research.[41] In our work, mechanical properties of PP/MAPP/30%CF achieved maximum values when the MAPP concentration was around 14 wt%. The over-addition of lower molecular weight MAPP (exceeding 14 wt%) would severely sacrifice the strength of the PP matrix.

For another, PP/MAPP/dCF presented the most outstanding mechanical performance. The flexural strength was increased by as high as 105.0%. Similarly, the flexural modulus was increased from 5.38 GPa to 9.00 GPa by 48.0% and impact strength from 6.82 KJ/m^2 to 22.03 KJ/m^2 by 223.0%, in reference to PP/CF. It was obvious that the improvement of mechanical performance through CF surface treatment was more significant in the presence of MAPP, in other words, MAPP and fiber modification had a good synergistic effect in strengthening interfacial interaction and a fascinating interface was formed between dCF reinforcement and PP/MAPP matrix.

In general, the obvious improvement on flexural and impact properties of PP/MAPP/dCF was greatly due to the important contribution of the increased wettability between fiber and matrix, the chemical bonding between amine groups and maleic anhydride groups as well as the hydrogen bonding interaction at the interface.

3.6 Fracture morphology of composites

The CF treatment by dopamine and matrix modification by MAPP helped improving the interfacial interaction was also confirmed by SEM. The fracture surface morphologies of PP/CF and PP/MAPP/dCF composites are shown in Fig. 12. In the case of PP/CF, it was observed that the CFs were aggregated slightly. Many holes were remained on the fracture due to the pull-out of fibers from the matrix under loading (Fig. 12a). The pulled-out CF presented a comparatively smooth surface without any remaining PP resin. Also, the gaps at the fiber/matrix boundary can be clearly observed (Fig. 12b), indicating that the fibers were debonded with PP matrix. As a consequence of the poor interfacial adhesion between the inert CFs and the low-polar PP, the failure and debonding firstly occurred in the weak interfacial region. While, the fracture region of PP/MAPP/dCF showed a sharply bright contrast, implying the property at the interface has been remarkably changed. On one hand, the holes almost disappeared (Fig. 12c). On the other hand, it is clear that the entire fiber surface were wrapped with a thin polymer layer and the fiber/matrix boundary was hard to distinguish (Fig. 12d), which was an evidence of strong bonding. In addition, most of fibers were well dispersed as individual ones in the matrix, which further proved the improved compatibility between dCFs and PP/MAPP resin. Such an enhanced interfacial adhesion would subsequently lead to a superior mechanical performance, which was in agreement with the

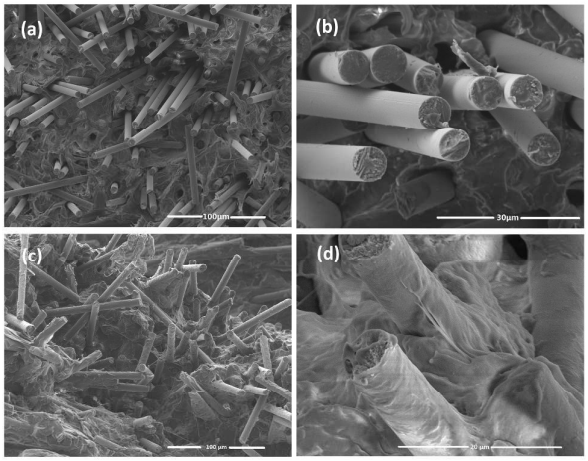

Fig. 12 SEM fracture micrographs of (a, b) PP/CF and (c, d) PP/MAPP/dCF composites (with 30 wt% CF)

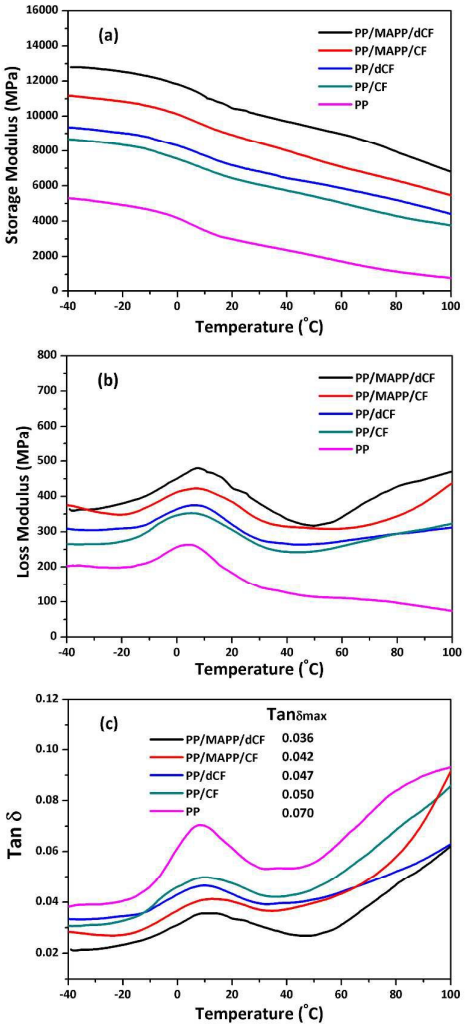

Fig. 13 DMA curves of neat PP and its composites (with 30 wt% CF) (a) storage modulus E´ (b) loss modulus E" (c) loss factor tan δ

above interfacial and mechanical properties.

3.7 Dynamic mechanical analysis of composites

Dynamic mechanical analysis (DMA) is based on the characteristic viscoelasticity of polymers. It is one of the effective ways to evaluate the interface of fiber reinforced composites. Three important parameters as a function of temperature can be obtained during periodic oscillations. Storage modulus (E´) is a measure of the energy stored in the material and also gives an idea of stiffness behavior of composites. Loss modulus (E") is proportional to the amount of dissipated energy. Tan δ is the ratio of loss modulus to storage modulus. It is related to the degree of molecular mobility in the composite material. Usually, strong interfacial fiber-matrix interaction induces a lower degree of polymer mobility and hence a lower tan δ value.[42]

The DMA curves of unfilled PP and its composites are presented in Fig. 13. The dynamic storage modulus E´ is approximately similar to the elastic modulus or the rigidity of materials. It was observed that the incorporation of 30 wt% CF into PP remarkably increased the E´ of PP composites. The E´ of PP/dCF, PP/MAPP/CF and PP/MAPP/dCF was continuously improved. This result was consistent with the flexural modulus data and could be attributed to the stiffening effect of CF.[43] Moreover, the better of the interfacial adhesion, the more enhancement was achieved as well as the higher E´ values. The loss modulus E" usually indicates the material's viscosity. As seen in Fig. 13b, the E" also increased with the addition of CF within the temperature range. Similarly, PP/MAPP/dCF showed the highest E". The interaction between fibers and matrix restricted the PP molecular movement, leading to a higher viscosity. Fig. 13c presents the temperature dependence of loss factor (tan δ) for PP and its composites. The temperature at the tan δ peak (tan δ_{max}) usually corresponds to the glass transition temperature (T_g). The damping in the glass transition region represented the energy dissipated for the deformation or irreversible intermolecular movement inside the materials.[44] It was noteworthy that the tan δ_{max} for PP composites dramatically shifted to lower values compared to that of neat PP (0.070). The tan δ_{max} of PP/CF, PP/dCF, PP/MAPP/CF and PP/MAPP/dCF were 0.050, 0.047, 0.042 and 0.036, respectively. The loss peaks were also gradually broadened. This indicated that the molecular mobility of PP segments in PP/MAPP/dCF composite was lowered, thus the less energy would be consumed to overcome the inter-friction between molecular chains and the relaxation time distribution was greater.[45] As a consequence of their interaction with fibre surface, This may contribute to the strongest chemical bonding between dCF and PP/MAPP matrix. As a result, DMA data was in accordance with the aforementioned mechanical results and once again proved the improvement effect of the PDA coating and MAPP addition for the PP composites.

4. Conclusions

In this study, bio-inspired PDA was used to functionalize CF through a facile dip-coating method, aimed to improve the interfacial interaction between CF and PP matrix. SEM, AFM and Raman confirmed that a uniform PDA layer was successfully coated on CF. IR and XPS demonstrated that more polar functional groups were introduced onto CF after functionalization. DCA results showed that PDA coating also increased the wettability and surface free energy of CF surface. As a consequence, the IFSS of dCF filament and PP/MAPP resin was dramatically enhanced from 4.84 MPa to 18.62 MPa by 282.3%. Similarly, PP/MAPP/dCF composite achieved the greatest advancements in macroscopic mechanical properties (e.g. flexural strength, flexural modulus and impact strength). Meanwhile, the storage modulus and loss modulus of PP/MAPP/dCF also showed notable improvement compared with PP/CF. The decrease of loss factor caused by the restricted molecular motion as well as SEM observations of

fracture morphology revealed the impressive interfacial adhesion between fibers and matrix. The greatly strengthened interfacial properties were largely due to the existence of PDA intermediate layer between the fiber and resin, which could bridge with MAPP in matrix through covalent and hydrogen bonding, thus contributing to the significantly increased bulk performance. We believe that using dopamine to modify CF surface was a promising way to improve the interfacial strength of CF reinforced various composites.

Acknowledgements

The authors thank for the financial support of Science and Technology Commission of Shanghai Municipality (Grant No. 12dz11004006).

References

1 C. Red, *Compos. Manuf.*, 2006, **7**, 24.
2 M. Q. Tran, K. K. C. Ho, G. Kalinka, M. S. P. Shaffer and A. Bismarck, *Compos. Sci. Technol.*, 2008, **68**, 1766.
3 F. Rezaei, R. Yunus, N. A. Ibrahim and E. S. Mahdi, *Polym-Plast. Technol. Eng.*, 2008, **47**, 351.
4 F. Rezaei, R. Yunus and N. A. Ibrahim, *Mater. Des.*, 2009, **30**, 260.
5 L. Shen, F. Q. Wang, H. Yang and Q. R. Meng, Polym. Test., 2011, **30**, 442.
6 J. Li and C. L. Cai, *Curr. Appl. Phys.*, 2011, **11**, 50.
7 J. H. Guo, C. X. Lu, F. An and S. Q. He, *Mater. Lett.*, 2012, **66**, 382.
8 Q. An, A. N. Rider and E. T. Thostenson, *Carbon*, 2012, **50**, 4130.
9 Z. Liu, C. Tang, P. Chen, Q. Yu and W. K. Li, *RSC Adv.*, 2014, **4**, 26881.
10 S. Rahmanian, K. S. Thean, A. R. Suraya, M. A. Shazed, M. M. Mohd Salleh and H. M. Yusoff, *Mater. Des.*, 2013, **43**, 10.
11 K. J. Kim, W. R. Yu, J. H. Youk and J. Y. Lee, *ACS Appl. Mater. Inter.*, 2012, **4**, 2250.
12 W. B. Liu, S. Zhang, L. F. Hao, F. Yang, W. C. Jiao, X. Q. Li and R. G. Wang, *Appl. Surf. Sci.*, 2013, **284**, 914.
13 J. S. Li, C. R. Zhang and B. Li, Appl. Surf. Sci., 2011, 257, 7752.
14 P. Agnihotri, S. Basu and K. K. Kar, *Carbon*, 2011, **49**, 3098.
15 H. J. Yuan, S. C. Zhang, C. X. Lu, S. Q. He and F. An, *Appl. Surf. Sci.*, 2013, **279**, 279.
16 X. Q. Zhang, H. B. Xu and X. Y. Fan, *RSC Adv.*, 2014, **4**, 12198.
17 L. C. Ma, L. H. Meng, Y. W. Wang, G. S. Wu, D. P. Fan, J. L. Yu, M. W. Qi and Y. D. Huang, *RSC Adv.*, 2014, **4**, 39156.
18 H. Lee, S. M. Dellatore, W. M. Miller and P. B. Messersmith, *Science*, 2007, **318**, 426.
19 P. Y. Sun, J. Wang, X. Yao, Y. Peng, X. X. Tu, P. F. Du, Z. Zheng and X. L. Wang, *ACS Appl. Mater. Inter.*, 2014, **6**, 12495.
20 S. L. Phua, L. Yang, C. L. Toh, D. Guoqiang, S. K. Lau, A. Dasari and X. H. Lu, *ACS Appl. Mater. Inter.*, 2013, **5**, 1302.
21 S. L. Phua, L. Yang, C. L. Toh, S. Huang, Z. Tsakadze, S. K. Lau, Y. W. Mai and X. H. Lu, ACS Appl. Mater. Inter., 2012, **4**, 4571.
22 L. P. Yang, S. L. Phua, J. K. H. Teo, C. L. Toh, S. K. Lau, J. Ma and X. H. Lu, *ACS Appl. Mater. Inter.*, 2011, **3**, 3026.
23 V. K. Thakur, D. Vennerberg and M. R. Kessler, *ACS Appl. Mater. Inter.*, 2014, **6**, 9349.
24 V. K. Thakur, J. Yan, M. F. Lin, C. Y. Zhi, D. Golberg, Y. Bando, R. Sim and P. S. Lee, *Polym. Chem.*, 2012, **3**, 962.
25 S. Ryu, Y. H. Lee, J. W. Hwang, S. Hong, C. Kim, T. G. Park, H. Lee and S. H. Hong, *Adv. Mater.*, 2011, **23**, 1971.
26 N. Gamze Karsli, A. Aytac, M. Akbulut, V. Deniz and O. Guven, *Radiat. Phys. Chem.*, 2013, **84**, 74.
27 K. H. Wong, D. S. Mohammed, S. J. Pickering and R. Brooks, *Compos. Sci. Technol.*, 2012, **72**, 835.
28 Y. W. Wang, L. H. Meng, L. Q. Fan, G. S. Wu, L. C. Ma and Y. D. Huang, *RSC Adv.*, **5**, 44492.
29 H. L. Wei, J. Ren, B. Han, L. Xu, L. L. Han and L. Y. Jia, *Colloid Surface B*, 2013, **110**, 22.
30 P. Y. Sun, J. Wang, X. Yao, Y. Peng, X. X. Tu, P. F. Du, Z. Zheng and X. L. Wang, *ACS Appl. Mater. Interf.*, 2014, **6**, 12495.
31 S. Hong, Y. S. Na, S. Choi, I. T. Song, W. Y. Kin and H. Lee, *Adv. Funct. Mater.*, 2012, **22**, 4711.
32 H. Yuan, C. G. Wang, S. Zhang and X. Lin, *Appl. Surf. Sci.*, 2012, **259**, 288.
33 F. Vautard, S. Ozcan, F. Paulauskas, J. E. Spruiell, H. Meyer and M. J. Lance, *Appl. Surf. Sci.*, 2012, **261**, 473.
34 S. Vollebregt, R. Ishihara, F. D. Tichelaar, Y. Hou and C. I. M. Beenakker, *Carbon*, 2012, **50**, 3542.
35 L. M. He, P. P. Zhao, Q. Han, X. Y. Wang, X. Cai, Y. F. Shi, L. B. Zhou, Y. M. Zhang and W. Xue, *Carbon*, 2013, **56**, 224.
36 D.W. Jiang, L. Liu, J. Long, L. X. Xing, Y. D. Huang, Z. J. Wu, X. R. Yan and Z. H. Guo, *Compos. Sci. Technol.*, 2014, **100**, 158.
37 Q. Y. Peng, Y. B. Li, X. D. He, H. Z. Lv, P. G. Hu, Y. Y. Shang, C. Wang, R. G. Wang, T. Sritharan and S. Y. Du, *Compos. Sci. Technol.*, 2013, **74**, 37.
38 Y. X. Li, Y. B. Li, Y. J. Ding, Q. Y. Peng, C. Wang, R. G. Wang, T. Sritharan, X. D. He and S. Y. Du, *Compos. Sci. Technol.*, 2013, **85**, 36.
39 Q. L. He, T. T. Yuan, S. Y. Wei and Z. H. Guo, *J. Mater. Chem. A*, 2013, **1**, 13064.
40 A. Arbelaiz, B. Fernandez, J. A. Ramos, A. Retegi, R. Llano-Ponte and I. Mondragon, *Compos. Sci. Technol.*, 2005, **65**, 1582.
41 Q. L. He, T. T. Yuan, X. R. Yan, D. W. Ding, Q. Wang, Z. P. Luo, T. D. Shen, S. Y. Wei, D. P. Cao and Z. H. Guo, *Macromol. Chem. Phys.*, 2014, **215**, 327.
42 M. Jacob, B. Francis, S. Thomas and K. T. Varughese, *Polym, Compos.*, 2006, **27**, 671.
43 N. G. Karsli and A. Aytac, Compos. B Eng., 2013, 51, 270.
44 S. Y. Li and D. G. Li, *Mater. Lett.*, 2014, **134**, 99.
45 M. Ragoubi, B. George, S. Molina, D. Bienaimé, A. Merlin, J.-M. Hive and A. Dahoun, *Compos. Part A*, 2012, **43**, 675.

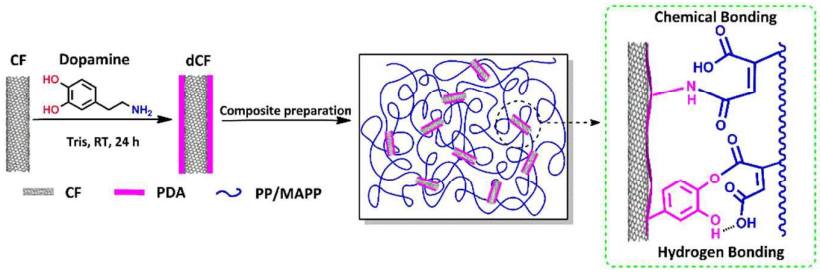

Carbon fiber was surface-functionalized by a facile dopamine self-polymerization to improve interfacial interaction with maleic anhydride grafted polypropylene modified PP